Lifetime of the recently identified 10^+ isomeric state at 3279 keV in the ^{136}Nd nucleus

A. Tucholski,[1] Ch. Droste,[2] J. Srebrny,[1] C. M. Petrache,[3] J. Skalski,[4] P. Jachimowicz,[5] M. Fila,[2] T. Abraham,[1] M. Kisieliński,[1] A. Kordyasz,[1] M. Kowalczyk,[1] J. Kownacki,[1] T. Marchlewski,[1] P. J. Napiorkowski,[1] L. Próchniak,[1] J. Samorajczyk-Pyśk,[1] A. Stolarz,[1] A. Astier,[3] B. F. Lv,[3] E. Dupont,[3] S. Lalkovski,[6] P. Walker,[7] E. Grodner,[4] and Z. Patyk[4]

[1]*Heavy Ion Laboratory, University of Warsaw, Pasteura 5a, 02-093 Warsaw, Poland*

[2]*Faculty of Physics, University of Warsaw, Pasteura 5, 02-093 Warszawa, Poland*

[3]*Centre de Sciences Nuclaires et Sciences de la Matire, CNRS/IN2P3, Université Paris-Saclay, Batiment 104-108, 91405 Orsay, France*

[4]*National Centre for Nuclear Research, Hoża 69, 00-681 Warsaw, Poland*

[5]*Faculty of Physics and Astronomy, University of Zielona Gora, Licealna 9, 65-417 Zielona Gora, Poland*

[6]*Nuclear Engineering, Faculty of Physics, Sofia University "St. Kl. Ohridski", 5 James Bourchier Boulevard, Sofia 1164, Bulgaria*

[7]*Department of Physics, University of Surrey, Guildford GU2 7XH, United Kingdom*

(Received 6 June 2019; published 31 July 2019)

Background: The γ softness of ^{136}Nd makes it possible to study the shape changes induced by two-proton or two-neutron excitation.

Purpose: We measure the lifetimes of two-quasiparticle states of the bands based on the 10^+ states at 3296 and 3279 keV to investigate the shape change induced by the alignment of two protons or two neutrons in the $h_{11/2}$ orbital.

Methods: The recoil-distance Doppler shift method was used for the study of ^{136}Nd studies, which was formed by the fusion reaction ^{120}Sn(^{20}Ne, $4n$)^{136}Nd, at $E_{beam} = 85$ MeV. Calculations were performed within the microscopic-macroscopic approach, based on the deformed Woods-Saxon single-particle potential and the Yukawa-plus-exponential macroscopic energy.

Results: The lifetime of the 10^+ state at 3279 keV of ^{136}Nd was measured to be $T_{1/2}^{10^+} = 1.63(9)$ ns. The lifetimes of the 2^+ state at 374 keV and of the 12^+ state at 3686 keV of the ground band were also measured to be $T_{1/2}^{2^+} = 26.5(14)$ ps and $T_{1/2}^{12^+} = 22.5(14)$ ps.

Conclusions: The measured lifetime of 10^+ the state at 3279 keV together with other observables confirm the structure change in ^{136}Nd. A rather small reduced hindrance of the electromagnetic decay of the 10^+ state at 3279 keV would be consistent with its K-mixed character.

DOI: 10.1103/PhysRevC.100.014330

I. INTRODUCTION

The study of transitional nuclei near closed shells provides detailed information on both collective behavior and particle excitation. This knowledge is especially important for low spin excitation where the nucleus can change into either prolate or oblate shape with small changes in excitation energy. In the current nucleus under study, ^{136}Nd, it can happen when a pair of nucleons in the $h_{11/2}$ orbit is broken. The comparison of two-quasi-proton and two-quasi-neutron excitation in nuclei is also interesting in the context of the latest studies of neutron rich nuclei since it provides complementary information on the origin of proton or neutron pairing and pair breaking. Proton rich nuclei can be routinely produced by fusion reactions with stable ions so that it becomes possible to collect sufficient statistics to determine the lifetimes of excited states which serve as tests of structure models.

The competition between two-proton and two-neutron excitation from the $h_{11/2}$ orbit in ^{136}Nd was discussed by Paul *et al.* in [1], where bands corresponding to the aligned two-proton $[h_{11/2}]^2$ and two-neutron $[h_{11/2}]^2$ configurations were identified. These two configurations were identified as corresponding to prolate and oblate shapes of this nucleus [2]. The two-proton and two-neutron S bands of ^{136}Nd have also been well reproduced by the interacting boson model plus broken pairs [3].

Previous in-beam spectroscopic studies of low- and medium-spin states in ^{136}Nd have developed the level scheme of this nucleus, as reported by Paul *et al.* [1] using the ^{116}Cd(^{24}Mg, $4n$)^{136}Nd reaction at bombarding energies of 106 and 111 MeV; by C.M. Petrache *et al.* [4–6] and S. Perries *et al.* [7] using the ^{110}Pd(^{30}Si, $4n$)^{136}Nd reaction at 130 MeV; by Billowes [8] using the ^{110}Pd(^{30}Si, $4n$)^{136}Nd reaction at 125 MeV; by Saito *et al.* [9] in relativistic Coulomb excitation; by Mergel *et al.* [10] using the ^{125}Te(^{16}O, $5n$)^{136}Nd reaction at 100 MeV; by S. Mukhopadhyay *et al.* [11] using the ^{100}Mo(^{40}Ar, $4n$)^{136}Nd reaction at 175 MeV; and by Lv *et al.* [12].

The present work reports lifetime measurements of the 10^+ state at 3279 keV of ^{136}Nd, the lifetimes of the 2^+ state at 374 keV, the 12^+ state at 3686 keV, and the upper limits of 12^+ (3997) and 11^- (4028) states, produced by the ^{120}Sn(^{20}Ne, $4n$)^{136}Nd reaction.

II. EXPERIMENTAL SETUP

The low-lying states of ^{136}Nd were populated via the ^{120}Sn(^{20}Ne, $4n$)^{136}Nd reaction and their decay was studied using the recoil-distance Doppler shift (RDDS) method with a plunger device. The ^{20}Ne beam at an energy of 85 MeV was produced by the U-200P cyclotron at the Heavy Ion Laboratory in Warsaw. This reaction at the energy of 85 MeV (close to the Coulomb barrier) was chosen because it has the highest cross section for ^{136}Nd production compared with other possible channels, and the reaction excites relatively low lying states, which guarantees the feeding of the searched for isomers. Our simulation program COMPA [13] shows that the maximum angular momentum of the entry state distribution corresponds to the spin $I = 17\hbar$, again indicating population of the 10^+ isomers. The ^{120}Sn target (0.5 mg/cm^2 thick) was evaporated on a Au supporting foil of 5 mg/cm^2 thickness. To stop the recoils, a second Au foil of 10 mg/cm^2 thickness was used. The plunger device was centered inside the EAGLE array [14] consisting of 16 high-purity germanium (HPGe) detectors, each one surrounded by an anti-Compton shield and collimator. The Ge detectors were positioned in rings at each of four angles with respect to the beam axis: 37° (5 detectors), 63° (4 detectors), 79° (4 detectors), and 143° (3 detectors). Data were recorded at 13 distances in the plunger device, ranging from 74 μm to 5 mm.

III. DATA ANALYSIS

The gamma spectra were collected in γ-γ coincidence mode when at least two γ rays registered in the detectors. Singles γ spectra were also collected. The down-scale factor was 1/10. A ^{152}Eu source was used for the efficiency calibration. The detector energy calibrations were made by using the γ lines of ^{136}Nd. The average recoil velocity $v = 1.03(3)\%\ c$ was determined experimentally from the energy spectra by measuring the distance between the stop and in-flight peaks. The half-lives of the isomeric 10^+ state at 3279 keV, the 12^+ state at 3686 keV, and the 2^+ state at 374 keV were measured (see Fig. 1) by the recoil-distance Doppler shift method.

As a monitor, the 1171 keV γ-rays coming from the Coulomb excited first 2^+ level in the ^{120}Sn target were used because of its high yield in the singles spectra. The second reason for using this monitor is that it has a very short half-life ($T_{1/2} = 0.5$ ps) which means that all excited ^{120}Sn nuclei decay in the vicinity of the target.

During the experiment the target-stopper distance was changed over the large range of 74 μm to 5 mm. That means that the target was seen by the Ge detectors under slightly different angles and distances. By analyzing the I_γ(monitor, $\theta = 37°$)/I_γ(monitor, $\theta = 143°$) ratio it was found that within the limit of the experimental errors there is no need to correct the detection efficiency for different target-stopper distances below 5 mm.

It was also found, by studying the ratio I_γ(flight 646 keV, $\theta = 37°$)/I_γ(flight+stop 646 keV, $\theta = 79°$) as a function of the target-to-stopper distance, that there is no need to correct gamma spectra for the deorientation effect for distances $d = 74$ μm to 5 mm which correspond to flight times $t = 24$ ps to 1.6 ns. This fact was used in the analysis of the 10^+ state of interest in this work.

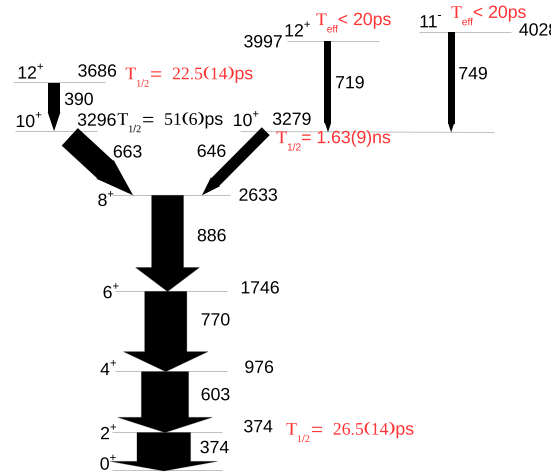

FIG. 1. Partial level scheme of ^{136}Nd. The half-lives are from the present experiment (red symbols) except for the 3296 keV level of $T_{1/2} = 51(6)$ ps, taken from Ref. [8].

The half-life of the 10^+, 3279 keV level (Fig. 1) was determined from the 646 keV γ line observed at $\theta = 37°$. This line and the neighboring 639 keV line (see the upper panel of Fig. 2) are visible in the γ-γ coincidence spectra

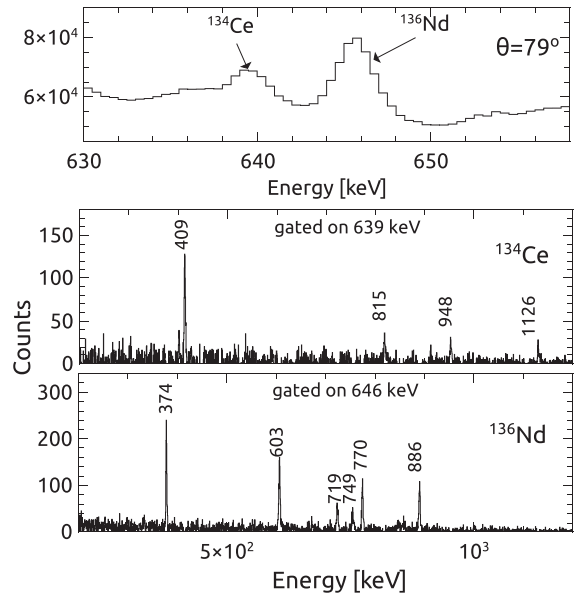

FIG. 2. The uppermost panel shows a γ-γ coincidence spectrum where both photons were registered in detectors located in the $\theta = 79°$ ring. The middle panel shows a γ-ray spectrum gated on the 639 keV line (coming from ^{134}Ce) and the lower panel shows a γ-ray spectrum gated on the line 646 keV (coming from ^{136}Nd). The spectra from the middle and lower panels show that the 639 and 646 keV lines come from the ^{134}Ce and ^{136}Nd nuclei, respectively. The 79° ring spectra were chosen because the small value of the Doppler shift energy difference, equal to 1.2 keV, allows the decay lines to be easily identified.

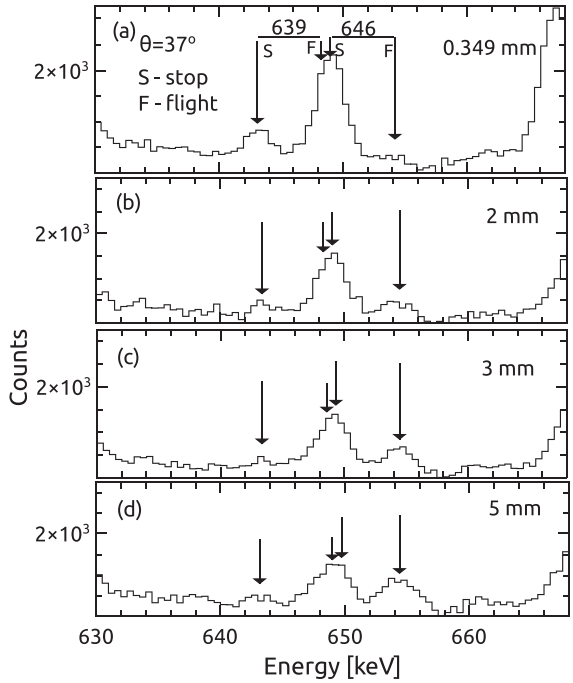

FIG. 3. The singles spectra of γ rays near 646 keV as a function of target-stopper distance. The relation between target-to-stopper distance and flight time is the following: 1 ps = 3.09 μm. The arrows mark the stop and in-flight peak from the ^{134}Ce $4^+ \rightarrow 2^+$, 639 keV transition and the stop and in-flight lines from the ^{136}Nd $10^+ \rightarrow 8^+$, 646 keV transition.

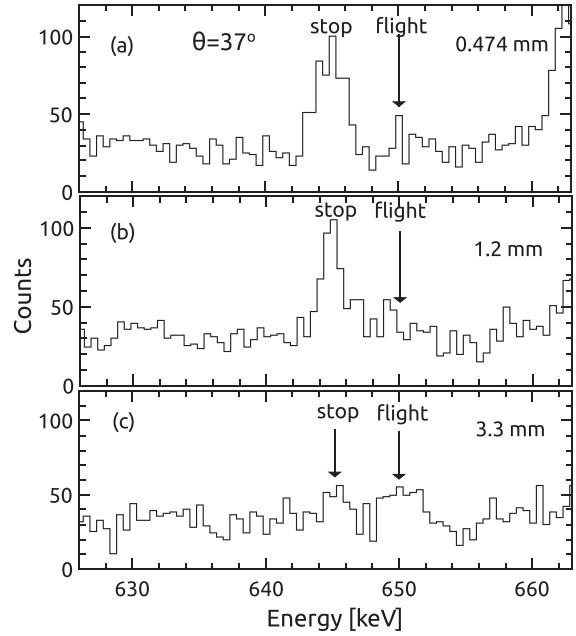

FIG. 4. The summed γ-rays spectra for the $10^+ \rightarrow 8^+$, 646 keV transition gated on the $2^+ \rightarrow 0+$, $4^+ \rightarrow 2^+$, or $6^+ \rightarrow 4^+$ transitions of the ground band from ^{136}Nd. Only the 646 keV flight and stop peaks are present.

registered in the 79° ring. At this angle the stopped and in-flight 646 keV peaks overlap since the energy difference of 1.2 for the 646 keV decay is below our detector resolutions, which were of the order of 2.5 keV on average.

It was found that the peak at 639 keV corresponds to the $4^+ \rightarrow 2^+$ transition in ^{134}Ce produced in the ^{120}Sn(^{20}Ne, $\alpha 2n$) reaction. If we set the gate on the 639 keV line, the known ^{134}Ce spectrum is obtained; see the middle panel of Fig. 2. If the gate is on the 646 keV line, the ^{136}Nd spectrum is observed (lower panel in Fig. 2), confirming our identification of this nucleus.

In Figs. 3 and 4 one can see the growing flight peak belonging to the 646 keV transition with growing distance in the plunger device. The 646 keV peak consists of two components: the stopped component of the $10^+ \rightarrow 8^+$, 646 keV transition in ^{136}Nd, and the other from the flight component of the $4^+ \rightarrow 2^+$ transition in ^{134}Ce. At a distance of around 350 μm (equivalent to 113 ps) there is almost no flight peak of ^{134}Ce and only the stopped peak of ^{136}Nd is visible. At 5 mm distance (1.6 ns) one can see the large flight component of the 646 keV line. The γ-γ coincidence spectra in Fig. 4 show the growing flight peak of the 646 transition, the same as that observed in the singles spectra in Fig. 3.

It follows from the level scheme given in Fig. 1 that there are two feeding transitions of the considered 10^+ state. One is the $12^+ \rightarrow 10^+$, 719 keV transition from the 3997 keV level, and the other is the $11^- \rightarrow 10^+$, 749 keV transition from the 4028 keV level. In both cases only flight components were observed for all target-stopper distances, which suggests that the effective half-lives of both states are below 14 ps. This observation gives us the possibility of extracting the half-life of the 10^+ (3279 keV) state straight from its decay to 8^+ (2633 keV). In further analysis of the 10^+ state, we used the singles spectra registered at $\theta = 37°$ and the 646 keV flight peak.

In Fig. 5, one can see the experimental intensities of the flight component of the $10^+ \rightarrow 8^+$ transition ($E_\gamma = 646$ keV) and its fitted decay curve. The measured half-life is $T_{1/2} =$ 1.63(9) ns.

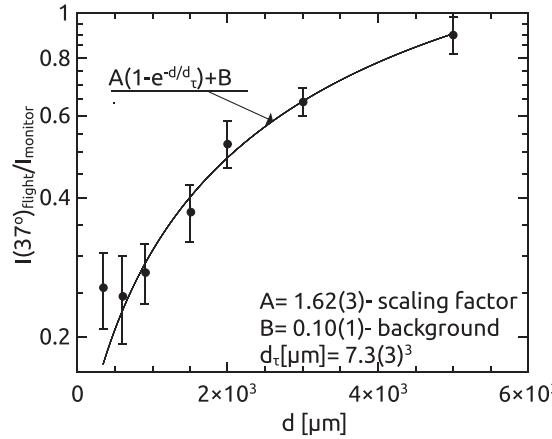

FIG. 5. The decay curve of the form $A(1 - e^{-d/d(\tau)}) + B$ fitted to the flight component of the $10^+ \rightarrow 8^+$, 646 keV transition in ^{136}Nd vs distances (d) in the plunger device. The resulting fit gives $T_{1/2} =$ 1.63(9) ns.

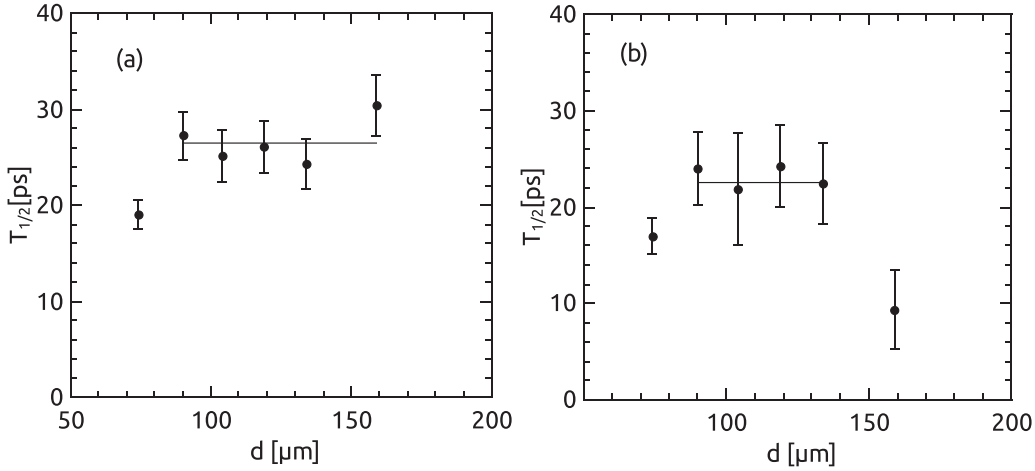

FIG. 6. Half-lives of the 2^+, 374 keV (a) and 12^+, 3686 keV (b) states of ^{136}Nd as a function of distances. The horizontal lines correspond to $T_{1/2}^{2^+} = 26.5(14)$ ps and $T_{1/2}^{12^+} = 22.5(14)$ ps. The horizontal lines include only the points of the sensitive region where the flight and stopped curves are far from saturation [18].

The recoil-distance Doppler shift (RDDS) method [15,16] was used to measure the half-lives of the excited 2^+ (374 keV) and 12^+ (3686 keV) states in ^{136}Nd. The half-lives of these levels were deduced from the differences in intensities of the flight and stopped peaks as a function of the distance between target and stopper and with the coincidence condition that the flight component of the transition feeding the considered level. In the RDDS method the half-lives derived are not affected by the deorientation phenomenon [17].

To measure the half-life of the first 2^+ state at 374 keV, the gate was set on the in-flight component of the $4^+ \rightarrow 2^+$, 603 keV transition (see Fig. 1). For the $12^+ \rightarrow 10^+$ transition, the coincidence with the in-flight line of the $14^+ \rightarrow 12^+$ transition was used. The measured half-lives as a function of distance are shown in Fig. 6. For the 2^+ state of the ground-state (g.s.) band we obtained $T_{1/2} = 26.5(14)$ ps [Fig. 6(a)] and for the 12^+ state at 3686 keV the half-life was found to be $T_{1/2} = 22.5(14)$ ps [Fig. 6(b)]. The $B(E2)$ value for the $2^+ \rightarrow 0^+$ transition measured in the relativistic Coulomb excitation experiment [9] was 80(11) W.u., which corresponds to $T_{1/2} = 23(3)$ ps, in good agreement with presented value of $T_{1/2} = 26.5(14)$ ps. All results concerning the half-lives ($T_{1/2}$) and reduced transition probabilities [$B(E(\lambda))$] are presented in Tables I and II.

TABLE I. Measured half-lives of the ^{136}Nd excited states.

E^{level} (keV) [a]	I^π	E_γ (keV)	$T_{1/2}$ (ps)
374	2^+	374	26.5(14)
3279	10^+	646	1630(90)
3686	12^+	390	22.5(14)
3997	12^+	719	< 14 [b]
4028	11^-	749	< 14 [b]

[a]References [1,4,8].
[b]Effective half-lives are given.

IV. DISCUSSION OF RESULTS

We performed calculations within the microscopic-macroscopic approach, based on the deformed Woods-Saxon single-particle potential [19] and the Yukawa-plus-exponential macroscopic energy [20]. Pairing constants were adopted from [21]. Admitted collective degrees of freedom include standard quadrupole deformations β and γ, hexadecapoles β_{40}, β_{42}, and β_{44}, and higher parity-preserving multipoles β_{60} and β_{80} (the latter two prohibit the full symmetry with respect to the $\gamma = 60^\circ$ line in Fig. 7). In Fig. 7 we show the energy landscape of ^{136}Nd at spin zero. It may be seen that the seven-dimensional minimization produces the g.s. minimum at triaxial deformation $\beta_{20} = 0.175$, $\beta_{22} = 0.077$, that corresponds to $\beta = 0.192$ and $\gamma = 23.8^\circ$ (the relation of β_{20} and β_{22} to β and γ is $\beta = \sqrt{\beta_{20}^2 + \beta_{22}^2}$, $\gamma = \arctan \beta_{22}/\beta_{20}$).

In Figs. 8 and 9 we show single particle (s.p.) levels as a function of triaxiality γ, with $\beta = 0.192$ (as in the triaxial minimum), and other deformations fixed by the energy minimization at each (β, γ). By looking at prolate and oblate sides of the s.p. spectrum one can notice that there are two possible, relatively low-lying two-quasiparticle $K^\pi = 10^+$ configurations: one neutron and one proton, both built from the orbitals $\Omega^\pi = 9/2^-$ and $11/2^-$ of the intruder $h_{11/2}$ subshells. The proton configuration is relatively low-lying at the oblate deformation, while the neutron one is relatively low-lying at the prolate deformation; their excitations above the triaxial minimum, calculated as the sum of deformation and two-quasiparticle energies, are equal to 3.5 and 3.05 MeV respectively. The calculations with blocking levels that for $\gamma \neq 0$ are continuations of $\Omega^\pi = 11/2^-$ and $9/2^-$ at the axial symmetry (up to the first crossing) show that the two-quasineutron configuration does not have a prolate minimum but a substantially triaxial one, while only a very shallow oblate minimum occurs for the two-quasiproton configuration.

As might be seen in Figs. 8 and 9, the orbitals $\Omega^\pi = 11/2^-$ and $9/2^-$ change to $1/2^-$ and $3/2^-$, respectively, when going

TABLE II. Electromagnetic transition strengths in ^{136}Nd.

E^{level} (keV)	$I_i \to I_f$[a]	E_γ (keV)	Multipolarity	$B(E\lambda)$ (e^2b^λ)	$B(E\lambda)$ (W.u.)
374	$2^+ \to 0^+$	374	$E2$	0.28(2)	68(4)
3279	$10^+ \to 8^+$	646	$E2$	0.00031(2)	0.073(4)
3686	$12^+ \to 10^+$	390	$E2$	0.27(2)	66.8(42)
3997	$12^+ \to 10^+$	719	$E2$	> 0.021	> 5.1
4028	$11^- \to 10^+$	749	$E1$	$>7.4^{-07}$	$>4.4^{-05}$

[a]References [1,4,8].

from prolate to oblate deformation for neutrons, and from oblate to prolate for protons. These lowest-Ω members of the $h_{11/2}$ intruder subshells lie much closer (less than 0.5 MeV) to the respective Fermi levels. With an increasing frequency of the collective rotation, such orbitals are expected to align their angular momenta with the rotation axis (rotational alignment), which gives rise to two S bands crossing the g.s. band. The alignment occurs at the rotational frequency controlled by the pairing gaps and $|\epsilon_\nu - \lambda|$, the distance of low-Ω $h_{11/2}$ orbitals ϵ_ν from the Fermi level λ. The deformation of the aligned configuration is driven towards the smaller $|\epsilon_\nu - \lambda|$, thus towards oblate collective rotation ($\gamma \approx -60^\circ$ in the Lund convention) for the aligned neutrons and towards collective prolate rotation ($\gamma \approx 0^\circ$) for the aligned protons.

The measurement of the magnetic moment of the 10^+ state at 3296 keV [12] indicates its aligned proton pair structure, which, together with the analysis of alignment in various bands [1], suggests that $h_{11/2}$ protons align before the neutrons do.

The interpretation of two other 10^+ states (3553 keV and 3279 keV) is not straightforward due to the softness to triaxiality of the ^{136}Nd nucleus and the proximity of their energies. In particular, the energy competition between the high-K and collectively rotating, low-K, aligned configurations depends on the actual γ-dependent Ω mixing. The 10^+ state at 3279 keV could be a configuration with two aligned $h_{11/2}$ neutrons at a negative γ, as suggested by cranking calculations without pairing in the recent work [12] (the band built on this state is referred to as L7 there). Then it would be strongly K mixed and one could argue that a more sophisticated model which preserves angular momentum should be used for its description; see the study [22] in this context. Another possibility for the 3279 keV state could be an only slightly K-mixed two-proton high-K configuration, although its estimated excitation is too high, and oblate high-K states rarely appear as bandheads for collective rotational bands. Either way, the noncollective character of the 646 keV, $E2$ transition (with a Weisskopf hindrance factor of $F_W = 14$, as measured in this work) suggests a substantial structural rearrangement, which could be due to the influence of the K quantum number, or to a shape change, or both.

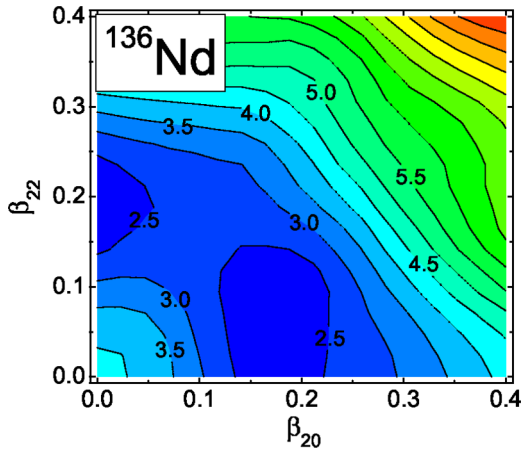

FIG. 7. Energy landscape of ^{136}Nd at spin zero.

V. SUMMARY

The lifetime of the isomeric state 10^+ at 3279 keV of ^{136}Nd was measured to be $T_{1/2}^{10^+} = 1.63(9)$ ns. The lifetimes of the

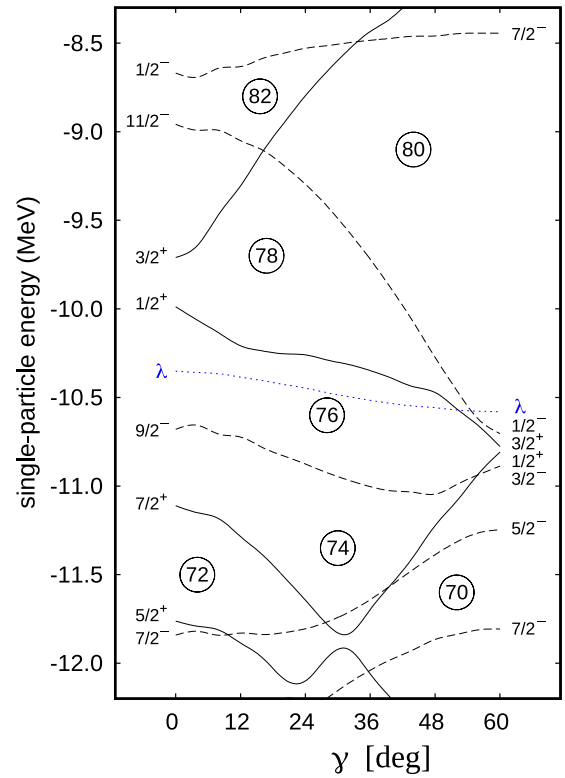

FIG. 8. Neutron s.p. energies in ^{136}Nd vs nonaxiality γ at $\beta = 0.192$. Full lines: positive parity; dashed lines: negative parity; short-dashed (blue)line: neutron Fermi level. For further details see text.

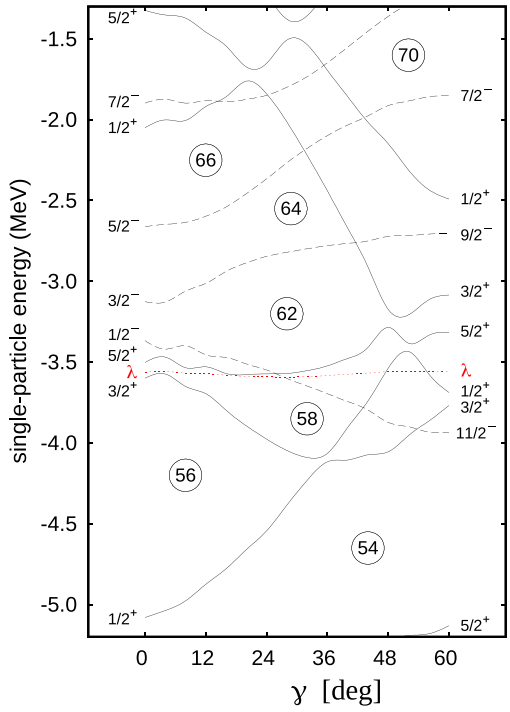

FIG. 9. Proton s.p. energies in ^{136}Nd vs nonaxiality γ at $\beta = 0.192$. Full lines: positive parity; dashed lines: negative parity; short-dashed (red) line: proton Fermi level. For further details see text.

2^+ state at 374 keV and of the 12^+ state at 3686 keV of the ground band were also measured to be $T^{2^+}_{1/2} = 26.5(14)$ ps and $T^{12^+}_{1/2} = 22.5(14)$ ps. The result $T_{1/2} = 1.63(9)$ ns gives $B(E2) = 0.073$ W.u. The nucleus ^{136}Nd has two 10^+ statesm at energies of 3296 and 3279 keV, with the reduced matrix elements $B(E2)$ of the $10^+ \rightarrow 8^+$ transition equal to $B(E2) = 2.09$ W.u. and $B(E2) = 0.073$ W.u., respectively. The ratio of the above reduced matrix elements is about 5.4. On the other hand the final 8^+ state is the same for both transitions. The density of states is very similar in both cases as the transition energies are almost the same.

A rather small reduced hindrance of the electromagnetic decay of the 10^+ state at 3279 keV, $f_\nu = 1.4$ for $\nu = 8$, would be consistent with its K-mixed character. The moment of inertia of the band built on it [1,12], smaller than the one of the g.s. band, would be compatible either with a decrease in β deformation for a two-neutron configuration or with a close-to-oblate deformation of the two-proton one.

ACKNOWLEDGMENTS

We are especially grateful to Prof. K. Kemper for careful reading of the manuscript and fruitful discussions with him. The work was supported by GAMMAPOOL European resources. This project has received funding from the European Union's Horizon 2020 research and innovation program under Grant Agreement No. n654002 and by Grant No. DEC-2013/10/M/ST2/00427 of the National Science Center. This work has been partly supported by the Polish-French COPIN-IN2P3 Collaboration agreement under Project No. 15-149. P.W. acknowledges support from the UK Science and Technology Facilities Council.

[1] E. S. Paul, C. W. Beausang, D. B. Fossan, R. Ma, W. F. Piel, Jr., P. K. Weng, and N. Xu, Phys. Rev. C **36**, 153 (1987).
[2] R. A. Wyss, A. Johnson, J. Nyberg, R. Bengtsson, and W. Nazarewicz, Z. Phys. A **329**, 255 (1988).
[3] D. Vretenar, S. Brant, G. Bonsignori, L. Corradini, and C. M. Petrache, Phys. Rev. C **57**, 675 (1998).
[4] C. M. Petrache *et al.*, Phys. Rev. C **53**, R2581 (1996).
[5] C. M. Petrache *et al.*, Phys. Lett. B **373**, 275 (1996).
[6] C. M. Petrache, Phys. Scr. **90**, 114016 (2015).
[7] S. Perries *et al.*, Phys. Rev. C **60**, 064313 (1999).
[8] J. Billowes, K. P. Lieb, J. W. Noe, W. F. Piel, S. L. Rolston, G. D. Sprouse, O. C. Kistner, and F. Christancho, Phys. Rev. C **36**, 974 (1987).
[9] T. R. Saito *et al.*, Phys. Lett. B **669**, 19 (2008).
[10] E. Mergel *et al.*, Eur. Phys. J. A **15**, 417 (2002).
[11] S. Mukhopadhyay, D. Almehed, U. Garg, S. Frauendorf, T. Li, P. V. Madhusudhana Rao, X. Wang, S. S. Ghugre, M. P. Carpenter, S. Gros, A. Hecht, R. V. F. Janssens, F. G. Kondev, T. Lauritsen, D. Seweryniak, and S. Zhu, Phys. Rev. C **78**, 034311 (2008).
[12] B. F. Lv *et al.*, Phys. Rev. C **98**, 044304 (2018).
[13] J. J. Mierzejewski, A. A. Pasternak, M. Komorowska, J. Srebrny, E. Grodner, and M. Kowalczyk, http://www.old.slcj.uw.edu.pl/pl/experiments/eagle/jan_mierzejewski_dr.pdf.
[14] J. Mierzejewski *et al.*, Nucl. Instrum. Methods **659**, 84 (2011).
[15] T. K. Alexander and A. Bell, Nucl. Instrum. Methods **81**, 22 (1970).
[16] P. Petkov *et al.*, Nucl. Phys. A **589**, 341 (1995); see also F. Naqvi *et al.*, Phys. Lett. B **728**, 303 (2014).
[17] P. Petkov, Nuclear Instruments and Methods in Physics Research Section A **349**, 289 (1994).
[18] A. Dewald, S. Harissopulos, and P. von Brentano, Z. Phys. A **334**, 163 (1989).
[19] S. Cwiok, J. Dudek, W. Nazarewicz, J. Skalski, and T. Werner, Comput. Phys. Commun. **46**, 379 (1987).
[20] H. J. Krappe, J. R. Nix, and A. J. Sierk, Phys. Rev. C **20**, 992 (1979).
[21] J. Dudek, A. Majhofer, and J. Skalski, J. Phys. G **6**, 447 (1980).
[22] J. A. Sheikh, G. H. Bhat, K. Palit, Z. Naik, and Y. Sun, Nucl. Phys. A **824**, 58 (2009).